doi:10.1093/brain/awu045 Brain 2014: 137; 1454–1469 | 1454

BRAIN
A JOURNAL OF NEUROLOGY

DARC shuttles inflammatory chemokines across the blood–brain barrier during autoimmune central nervous system inflammation

Carsten Minten,[1,*] Carsten Alt,[1,†] Melanie Gentner,[2] Elisabeth Frei,[1] Urban Deutsch,[1] Ruth Lyck,[1] Nicole Schaeren-Wiemers,[2] Antal Rot[3] and Britta Engelhardt[1]

1 Theodor Kocher Institute, University of Bern, CH-3012 Bern, Switzerland
2 Neurobiology, Department of Biomedicine, University Hospital Basel, University Basel, Switzerland
3 MRC Centre for Immune Regulation, School of Immunity and Infection, University of Birmingham, UK

*Present address: Olympus Australia, Australia
†Present address: Palo Alto Institute for Research and Education, Veterans Affairs Palo Alto Health Care System, Palo Alto, CA, USA

Correspondence to: Britta Engelhardt,
University of Bern,
Theodor Kocher Institute,
Freiestr. 1,
CH-3012 Bern, Switzerland
E-mail: bengel@tki.unibe.ch

The Duffy antigen/receptor for chemokines, DARC, belongs to the family of atypical heptahelical chemokine receptors that do not couple to G proteins and therefore fail to transmit conventional intracellular signals. Here we show that during experimental autoimmune encephalomyelitis, an animal model of multiple sclerosis, the expression of DARC is upregulated at the blood–brain barrier. These findings are corroborated by the presence of a significantly increased number of subcortical white matter microvessels staining positive for DARC in human multiple sclerosis brains as compared to control tissue. Using an *in vitro* blood–brain barrier model we demonstrated that endothelial DARC mediates the abluminal to luminal transport of inflammatory chemokines across the blood–brain barrier. An involvement of DARC in experimental autoimmune encephalomyelitis pathogenesis was confirmed by the observed ameliorated experimental autoimmune encephalomyelitis in *Darc*$^{-/-}$ C57BL/6 and SJL mice, as compared to wild-type control littermates. Experimental autoimmune encephalomyelitis studies in bone marrow chimeric *Darc*$^{-/-}$ and wild-type mice revealed that increased plasma levels of inflammatory chemokines in experimental autoimmune encephalomyelitis depended on the presence of erythrocyte DARC. However, fully developed experimental autoimmune encephalomyelitis required the expression of endothelial DARC. Taken together, our data show a role for erythrocyte DARC as a chemokine reservoir and that endothelial DARC contributes to the pathogenesis of experimental autoimmune encephalomyelitis by shuttling chemokines across the blood–brain barrier.

Keywords: DARC; chemokines; blood–brain barrier; multiple sclerosis; experimental autoimmune encephalomyelitis

Abbreviations: EAE = experimental autoimmune encephalomyelitis; pMBMEC = primary mouse brain microvascular endothelial cell

Received October 21, 2013. Revised December 30, 2013. Accepted January 14, 2014. Advance Access publication March 12, 2014

Introduction

Multiple sclerosis is the most common inflammatory demyelinating disease of the CNS with unknown aetiology to this date. Much of our current knowledge about multiple sclerosis pathogenesis has been obtained from its animal model experimental autoimmune encephalomyelitis (EAE). In EAE $CD4^+$ auto-aggressive T cells are activated outside of the CNS. To gain access to the CNS, where they start the molecular events leading to inflammation, oedema formation and demyelination, T cells have to breach the endothelial blood–brain barrier. Interaction of auto-aggressive immune cells with the blood–brain barrier endothelium has therefore been recognized as a major pathophysiological hallmark of EAE and multiple sclerosis. In fact, inhibition of immune cell trafficking into the CNS with the humanized anti-α4-integrin antibody natalizumab is a successful therapeutic regimen for the treatment of multiple sclerosis (Engelhardt and Kappos, 2008).

The recruitment of T cells across the inflamed blood–brain barrier during EAE is mediated by the sequential interaction of different adhesion and/or signalling molecules on the immune cell and the blood–brain barrier endothelium. P-selectin/PSGL-1-mediated rolling and α4β1-integrin/VCAM1-mediated capture of encephalitogenic T cells on the brain endothelium is followed by α4β1-integrin-VCAM1 and LFA-1–ICAM1/2-mediated T cell arrest on the blood–brain barrier. This is followed by LFA-1-ICAM1/2 mediated T cell polarization and T cell crawling on the blood–brain barrier against the direction of blood flow with the aim to find a site permissive for diapedesis across the blood–brain barrier (Engelhardt and Ransohoff, 2012).

In addition to integrins and their endothelial ligands of the immunoglobulin superfamily there is a large body of evidence suggesting that chemokines are critically involved in the migration of inflammatory cells across the blood–brain barrier during EAE and multiple sclerosis. Chemokine binding to their respective G-protein coupled receptors on the leucocyte surface leads to the inside-out activation of constitutively expressed integrins on the leucocyte surface. Activated intergins display an increased affinity and avidity, which is prerequisite for integrin-mediated firm adhesion of immune cells to the vascular endothelium. Live cell imaging studies have provided evidence that integrin-mediated stable adhesion of encephalitogenic T cells in CNS microvessels requires G-protein coupled receptor signalling (Vajkoczy *et al*., 2001; Piccio *et al*., 2002). To act on the circulating T cells, the chemokines must be available at the luminal surface of the blood–brain barrier. Luminal presence of CCL2 and CCL5 on the blood–brain barrier has been suggested by live cell imaging studies demonstrating that antibodies blocking CCL2 and CCL5 prevented leucocyte adhesion but not rolling in the inflamed brain microvasculature during EAE (dos Santos *et al*., 2005). In addition, EAE studies in mice with genetic deletions of the chemokine receptors CCR1 (Rottman *et al*., 2000), CCR2 (Fife *et al*., 2000; Izikson *et al*., 2000) or CXCR2 (Carlson *et al*., 2008) have indicated that these molecules and their respective ligands—CCL5, CCL2 and CXCL1 (Roy *et al*., 2012)—are involved in EAE pathogenesis. In apparent contrast to their involvement in inflammatory cell entry into the CNS during EAE, expression of CCL2, CCL5 and CXCL1 was found to be mainly localized to astrocytes within the CNS parenchyma, rather than to brain endothelial cells (Ransohoff *et al*., 1993; Miyagishi *et al*., 1997; Glabinski *et al*., 1999). If these chemokines therefore function to mediate inflammatory cell entry into the CNS parenchyma during EAE it is mandatory that they could breach the endothelial blood–brain barrier from the abluminal to the luminal side.

In contrast to blood vessels in peripheral organs, the highly specialized endothelial cells forming the blood–brain barrier inhibit transcellular or paracellular diffusion of inflammatory mediators by their extremely low pinocytotic activity and an elaborate network of complex P-face associated tight junctions between the endothelial cells (Engelhardt and Sorokin, 2009). These physical barrier characteristics protect the CNS parenchyma from the constantly changing milieu in the blood stream and thus maintain CNS homeostasis, which is prerequisite for the proper function of neurons. At the same time the blood–brain barrier endothelium establishes a functional barrier by the expression of transporters and enzymes, which strictly control the import of nutrients from the blood stream into the CNS and the export or degradation of metabolites out of the CNS (Engelhardt and Sorokin, 2009). Thus, availability of inflammatory chemokines derived from CNS parenchymal cells on the luminal blood–brain barrier critically relies on the availability of a chemokine transport system allowing CNS expressed chemokines to breach the blood–brain barrier from the abluminal to the luminal side.

One such transport system could be the Duffy antigen receptor for chemokines (DARC). DARC belongs to a family of silent seven-transmembrane spanning receptors, which because of the lack of the DRYLAIV consensus motif in the second intracellular loop, do not couple to G proteins and therefore do not transmit intracellular signals like other G-protein coupled chemokine-receptors leading to integrin activation or cell motility (Novitzky-Basso and Rot, 2012). DARC binds to a broad range of inflammatory chemokines of both the CC and the CXC chemokine families, but does not interact with homeostatic chemokines (Gardner *et al*., 2004). DARC is expressed on erythrocytes, cerebellar neurons and most importantly on postcapillary venule and capillary endothelial cells in a number of peripheral organs including lymph nodes (Kashiwazaki *et al*., 2003), the lung (Lee *et al*., 2003), and the kidney, but not on arterial endothelial cells (Middleton *et al*., 2002). In these organs, endothelial DARC is therefore specifically expressed in the vascular segment involved in leucocyte extravasation. In fact, DARC was shown to mediate chemokine transcytosis from the basolateral to the luminal side of the endothelium, where the chemokines remain immobilized on the tips of endothelial apical microvilli and enhance leucocyte trafficking *in vivo* (Pruenster *et al*., 2009).

Expression of DARC at the blood–brain barrier has not been described. Here we investigated expression of DARC in blood–brain barrier endothelium. We found that DARC is induced in blood–brain barrier endothelium before onset of clinical EAE and in multiple sclerosis *in vivo* and that brain endothelial DARC can shuttle inflammatory chemokines from the abluminal to the luminal surface of an *in vitro* blood–brain barrier model. Contribution of DARC in EAE pathogenesis was confirmed by an ameliorated disease course in $Darc^{-/-}$ SJL/J and $Darc^{-/-}$ C57BL/

6 mice compared with wild-type littermates. EAE experiments in reciprocal bone marrow chimeric mice demonstrated that although increased plasma levels of inflammatory chemokines observed during EAE depended on the presence of erythrocyte DARC, amelioration of EAE required the absence of endothelial DARC. Taken together, our data confirm a role for erythrocyte DARC as a chemokine reservoir and demonstrate that endothelial DARC contributes to EAE pathogenesis by shuttling chemokines across the blood–brain barrier.

Materials and methods

Mice

Mice were bred in individually ventilated cages at specific pathogen-free conditions according to the animal protection law of the Kanton Bern, Switzerland. Breeding of mice and all animal experiments shown in this study have been approved by the veterinary office of the Kanton Bern. Wild-type SJL/J HanHsd (SJL) or C57BL/6 JOlaHsd (C57BL/6) mice were purchased from Harlan, AD Horst, The Netherlands. *Darc*$^{-/-}$ mice (Dawson *et al*., 2000) were characterized previously and shown to lack expression of functional DARC protein. *Darc*$^{-/-}$ mice were backcrossed into C57BL/6 or SJL background for a minimum of 10 generations before use in experiments. The genotype of mice was confirmed by PCR as described (Dawson *et al*., 2000).

Reciprocal bone marrow chimeric mice were generated by reconstituting lethally irradiated C57BL/6 or *Darc*$^{-/-}$ C57BL/6 mice (10 grey) with 1×10^6 up to 2.5×10^6 isolated total bone marrow cells of non-irradiated donor mice of either C57BL/6 wild-type or *Darc*$^{-/-}$ C57BL/6 mice. Recipient mice were used at 12 to 14 weeks of age and bone marrow donor mice were used at the age of 12 weeks to 6 months. After bone marrow reconstitution, mice were kept in individually ventilated cages on autoclaved bedding. Mice received trimethoprim (0.16 mg/ml) and sulfamethoxazole (0.8 mg/ml) within their drinking water as a precaution. Mice were used for experiments 6–8 weeks after reconstitution.

Human tissue

Human brain tissues were obtained from post-mortem autopsies supplied by the UK Multiple Sclerosis Tissue Bank (UK Multicentre Research Ethics Committee, MREC/02/2/39), funded by the Multiple Sclerosis Society of Great Britain and Northern Ireland (registered charity 207495). Cortical tissue with subcortical white matter from five cases without any diagnosed neurological disease was taken as controls. These subjects had an average age of 69.4 years [±21.5 standard deviation (SD)] and an average post-mortem time of autopsy was 14.2 h (±6.98 SD). Cortical tissues from nine cases with multiple sclerosis with average disease duration of 28.75 years (±11 SD) were used for this study. Their average age was 56 years (±15.98 SD), and an average post-mortem time of autopsy was 13.67 h (±6.73 SD).

DARC-positive blood vessels in subcortical white matter in multiple sclerosis and control cases were counted using the 'cell counter' in ImageJ and assessed per cm^2. An unpaired *t*-test was performed with the data for all multiple sclerosis cases ($n = 10$ tissue samples of nine cases) and control cases ($n = 8$ tissue samples of five cases).

Experimental autoimmune encephalomyelitis

Active EAE was induced in 8–12-week-old C57BL/6 wild-type and *Darc*$^{-/-}$ C57BL/6 mice or in bone marrow chimeric mice 6 to 8 weeks after reconstitutions, as described previously (Engelhardt *et al*., 2005; Doring *et al*., 2007). Active EAE in *Darc*$^{-/-}$ SJL and wild-type SJL mice was induced as described (Engelhardt *et al*., 2005; Doring *et al*., 2007). Weight and clinical disease were assessed daily and scored as: 0 = healthy, 0.5 = limb tail, 1 = hind leg weakness, 2 = hind leg paraplegia, 3 = hind leg paraplegia and incontinence. Mice with more severe EAE scores were sacrificed as requested by the veterinary office of the Kanton Bern and are therefore not included into this study.

Antibodies

Supernatants of the hybridomas Hermes-1 (9B5, anti-human CD44, used as an isotype-matched control) and M1/9 (anti-mouse CD45) were produced in our own laboratory and used undiluted. Mec13.3 (anti-mouse PECAM1) was a gift of Dr E. Dejana (IFOM, Milan, Italy). A polyclonal rabbit anti-mouse DARC antibody against the C-terminus (amino acids 319–333: LPRQASQMDALAGK) as previously published (Kashiwazaki *et al*., 2003) was prepared by Sigma-Genosys, Sigma Aldrich. Purified IgG fractions of the antisera were obtained by protein A affinity chromatography. Specific recognition of DARC by the polyclonal IgG fraction was confirmed by positive immmunoreactivity on spotted peptides, western blots of lymph nodes and specific staining of high endothelial venules of peripheral lymph nodes in frozen tissue sections of wild-type mice and absence of this staining in *Darc*$^{-/-}$ mice. Secondary antibodies used were Alexa Fluor® 488 goat-anti rat IgG, Cy3 goat anti rat IgG, biotin goat anti-rat IgG combined with AMCA-streptavidin and Cy3-goat anti rabbit IgG (all from Jackson ImmunoResearch Laboratories).

Immunofluorescence staining

Immunofluorscence staining of mouse tissue sections and on pMBMECs (primary mouse brain microvascular endothelial cells) were performed as described previously (Pfeiffer *et al*., 2008, 2011; Steiner *et al*., 2011).

Immunohistochemistry on human brain tissue

Cryostat sections (12 µm) of fresh frozen human post-mortem cortical tissue were fixed in 4% paraformaldehyde for 10 min at 4°C. For inactivation of endogenous peroxidise, sections were treated with 0.6% hydrogen peroxide in methanol for 30 min and blocked with blocking buffer (1% normal donkey serum, 0.1% Triton, 0.05% Tween) for 1 h. Sections were incubated with the following primary antibodies overnight at 4°C: mouse anti-human DARC (generous gift from Dr M. Uchikawa, Japanese Red Cross, Tokyo, Japan, 1:200), mouse anti-MOG (clone Z12, kindly provided by R. Reynolds, 1:100), mouse anti-CD68 (Abcam Ab845, 1:50) and mouse anti-CollagenIV (Cemicon, 1:2000). Secondary botinylated antibodies (Vector Laboratories, 1:500) were applied for 2 h at room temperature, followed by ABC complex reagent (Vector Labs) for 30 min. Colour reaction was performed with 3-amino-9-ethylcarbazole. Cells were stained in haematoxylin for 5 min and rinsed afterwards under running tap water.

In situ hybridization

In situ hybridization was performed as described (Alt *et al*., 2002). Briefly, single-stranded ^{35}S-labelled antisense or sense RNA-probes were generated by *in vitro* transcription using T3 or T7 RNA polymerases as described by the manufacturer (Stratagene). The probe for *in situ* hybridization was prepared from the I.M.A.G.E. Consortium (Lennon *et al*., 1996) complementary DNA Clone IMAGE:718084. The *Darc* complementary DNA EcoRI/NotI fragment was subcloned into pBluescript II KS+ (Stratagene). Expression of *Darc* messenger RNA was investigated in sections of brain and spinal cord derived from two different SJL/N mice with EAE (Day 14 and Day 17 post-immunization, clinical score 2 and 3, respectively) and from two different healthy age-matched control mice. Specificity of the hybridization signals was verified by the use of sense probes on serial control sections. After hybridization, slides were coated with photographic emulsion (Kodak NTB-2) and exposed for 4 weeks. After fixation, sections were counterstained with Toluidine blue, dehydrated, mounted and analysed with dark and bright field microscopy.

Quantitative polymerase chain reaction analysis

RNA extraction, complementary DNA synthesis and quantitative real-time PCR analysis using SYBR® Green were performed in triplicates as described (Lyck *et al*., 2009). The following primer pairs were used: Pair 1: primer 911 (5′-CTTCACCTTGGGACTCAGTGT-3′) and primer 912 (5′-GACTGGCAGCCCTAAGAGG-3′). Pair 2: primer 913 (5′-AGT GTCCTGGGCATGCTG-3′) and primer 914 (5′-CTGCCAGTGGAAGA AAGGTC-3′). Negative control complementary DNA samples without reverse transcriptase enzyme were assayed in parallel. As reference s16 ribosomal protein messenger RNA was included using the following primer pair: sense GATATTCGGGTCCGTGTGA; reverse TTGAGAT GGACTGTCGGATG.

T cell proliferation assay

In vitro antigen-recall assays to test for antigen-specific proliferation of T cells was determined by measuring ^{3}H-thymidine incorporation into the DNA of proliferating T cells as previously described (Engelhardt *et al*., 1998; Doring *et al*., 2007).

In vitro chemokine transport across the blood–brain barrier

For *in vitro* chemokine transcytosis, pMBMECs were isolated from brains of DARC-deficient and wild-type SJL mice at 6–8 weeks of age, as described (Steiner *et al*., 2010). pMBMECs plated on Matrigel (BD Biosciences) coated 0.4 μm pore size transwell filters (Corning; Vitaris AG) and cultured for 6 days to reach confluency. Optionally, pMBMECs were stimulated for 16–18 h with recombinant mouse TNF-α (12.5 ng/ml). Endothelial cell-derived chemokine production was assayed from samples taken before the experiments. pMBMECs were washed once in minimal assay medium [Dulbecco's modified Eagle medium (4500 g/l glucose), 5 % (v/v) newborn calf serum, 25 mM HEPES, 4 mM L-glutamine] and 100 μl fresh minimal assay media was applied to the upper chamber. Fifty nanograms per millilitre of the respective recombinant mouse chemokines (R&D Systems Europe Ltd) added to 600 μl minimal assay media into the lower chamber and incubated at 37°C, 10% CO_2. At 1-, 2- and 3-h time points the filter inserts were removed to stop chemokine transport and 50 μl samples were taken from the upper chambers and immediately frozen at −20°C. After addition of 50 μl fresh minimal assay media to the upper chamber, filter inserts were placed back into the lower compartment and the assay was further incubated until the next time point. At the 3-h time point the assay was stopped and 50 μl samples were taken from the upper and lower chambers. Filter inserts were washed twice in PBS, fixed for 2 h in formalin gas phase and Giemsa stained [10 % (v/v) Giemsa solution in tap water; Sigma Aldrich] for 30 min. Cells were air-dried overnight and mounted on glass slides. Endothelial monolayer confluency was analysed by light microscopy. All conditions were assayed in triplicates.

Detection of chemokines in mouse plasma

Mice were anaesthetized and blood was collected by retro-orbital bleed. Heparin (5000 U/ml) was added immediately and blood samples were centrifuged (3000*g*) for 15 min at 4°C. Translucent blood plasma was collected and stored at −20°C. Detection of chemokines in mouse plasma was performed using a mouse cytokine array (R&D Systems Europe Ltd) according to the instructions provided by the manufacturer.

Analysis of chemokine concentrations by ELISA

Chemokine concentrations in blood plasma or in samples from chemokine transcytosis assays were determined by ELISA (R&D Systems UK) according to the protocol provided by the manufacturer. Data were analysed using GraphPad Prism software, calculating values using a four-parameter sigmoidal curve fit model.

Permeability assay

Barrier function of pMBMEC monolayers was studied as described (Steiner *et al*., 2011).

Statistics

All statistical analyses were performed using Graph Pad Prism 4.0 software for Macintosh. If not indicated differently, data are presented as mean ± SD and Student's *t*-test was performed to compare different data sets. Asterisks indicate significant differences ($*P < 0.05$; $**P < 0.005$; $***P < 0.001$).

Results

Expression of DARC is induced in microvascular endothelial cells of the CNS before onset and during experimental autoimmune encephalomyelitis

In a previous gene expression profiling study aiming to identify genes involved in the migration of inflammatory cells across the blood–brain barrier during EAE, we identified upregulated expression of DARC in cerebral microvessel preparations from C57BL/6

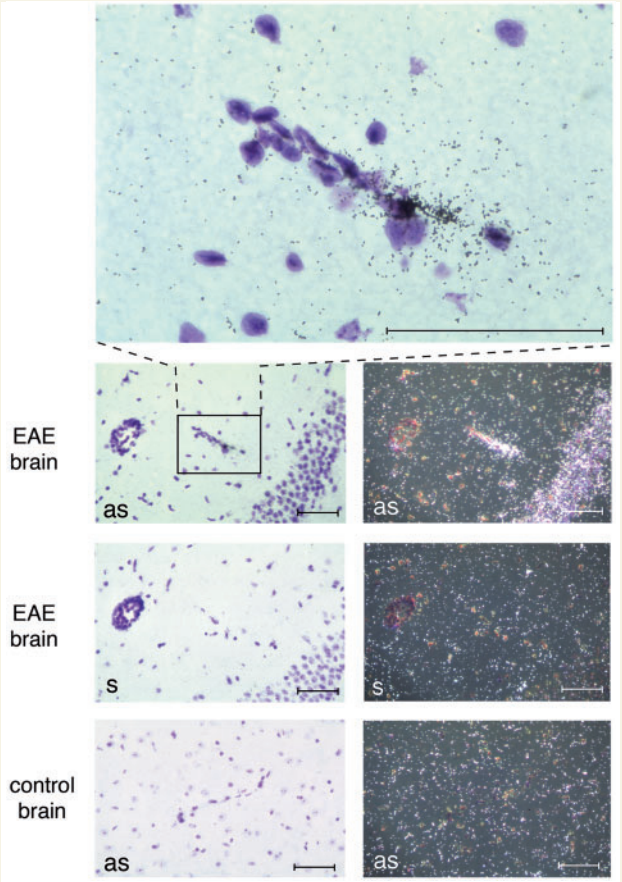

Figure 1 Induction of vascular *Darc* expression during EAE. *In situ* hybridization analysis for *Darc* in the cerebellum of an SJL mouse with EAE (Day 14, clinical score 2) and in a healthy control mouse. A specific hybridization signal for *Darc* can be localized to inflamed vessels in the EAE brain but not the control brain with the anti-sense (as) probe. Note the additional specific hybridization signal on cerebellar neurons of the granule cell layer in the right lower corner. Control *in situ* hybridization using the sense (s) probe did not produce any signal. Sections were counterstained with Toluidine blue. *Left*: Bright field images. *Right*: Dark field images. *Top*: Enlarged bright field image showing *Darc*-specific hybridization on inflamed brain vessel during EAE. Scale bar = 50 μm. One experiment out of two analysing two mice per group is shown.

and SJL mice with EAE when compared with microvessel preparations from healthy control mice (Alt *et al*., 2005). Subtractive suppression hybridization and subsequent sequencing corroborated induction of DARC in inflamed microvessels during EAE (Alt *et al*., 2005).

As DARC belongs to the family of atypical chemokine receptors, its upregulation in inflamed CNS microvessels during EAE suggested its involvement in the transport of CNS chemokines to the luminal surface of brain endothelial cells and consequent leucocyte recruitment across the blood–brain barrier (Pruenster *et al*., 2009). To localize DARC expression to the endothelial cells of CNS microvessels we performed *in situ* hybridizations on frozen brain sections of SJL mice with EAE and of healthy SJL mice. We found expression of *Darc* messenger RNA in brain endothelial cells of inflamed venules in mice suffering from EAE but not in the brains of healthy SJL mice (Fig. 1). We also confirmed expression of *Darc* messenger RNA in cerebellar neurons as previously described (Horuk *et al*., 1996).

To validate the expression of DARC in endothelial cells of inflamed CNS microvessels at the protein level, we generated a polyclonal rabbit anti-mouse DARC antibody. Immunofluorescence staining for DARC on frozen brain and spinal cord sections of SJL and C57BL/6 mice at different time points after induction of EAE was combined with staining for PECAM1 to identify endothelial cells and staining for CD45 to localize inflammatory cells. The first detectable immunofluorescent signal for DARC on PECAM1$^+$ endothelial cells of brain and spinal cord venules was already observed at Day 7 after induction of EAE in both C57BL/6 and SJL mice (Fig. 2, Supplementary Fig. 1 and data not shown). At that time clinical EAE had not yet started and only sparse CD45$^+$ inflammatory cells were present in the CNS. On Day 11 post-immunization at the onset of clinical EAE we observed immunofluorescence for DARC on PECAM1$^+$ endothelial cells of brain and spinal cord venules surrounded by CD45$^+$ inflammatory cell infiltrates. Additional immunofluorescence for DARC was observed on PECAM1$^+$ endothelial cells in venules not surrounded by inflammatory cells. At Day 13 or 14 post-immunization during ongoing EAE immunofluorescence for DARC was not further increased and restricted to venules surrounded by inflammatory cuffs (Fig. 2 and Supplementary Fig. 1). Taken together these findings suggest that expression of DARC is induced in endothelial cells of CNS venules after the induction of EAE before immune cell recruitment across the blood–brain barrier and might contribute to cellular infiltration of the CNS.

Increased expression of DARC in multiple sclerosis white matter

To investigate whether DARC is also expressed in multiple sclerosis, immunohistochemistry was performed on post-mortem multiple sclerosis brain tissues of nine cases with multiple sclerosis analysing chronic active and chronic inactive lesions and compared to five control cases without any diagnosed neurological disease. DARC-positive blood vessels were detected in inflammatory demyelinating lesions (Fig. 3B), identified by lack of myelin (Fig. 3A) and inflamed vessels (Fig. 3C), in meninges, and in normal appearing white matter in multiple sclerosis as well as in inflamed white matter microvessels of control cases characterized by the presence of CD68$^+$ macrophages/activated microglia (Fig. 3). Activated microglia in multiple sclerosis and control white matter is frequently observed in post-mortem brain tissue, but no direct correlation with DARC immunoreactivity could be identified. Comparison with collagen IV immunostaining (Fig. 3E), expressed by all CNS vessels, revealed DARC expression in a subset of microvessels in multiple sclerosis and in controls (Fig. 3F). Interestingly, control cases showing signs of neurodegenerative diseases other than multiple sclerosis accompanied by chronic inflammation such as Alzheimer's disease (detection of tau aggregates) or hypoxia also presented with increased numbers of DARC$^+$ brain microvessels (data not shown). When excluding

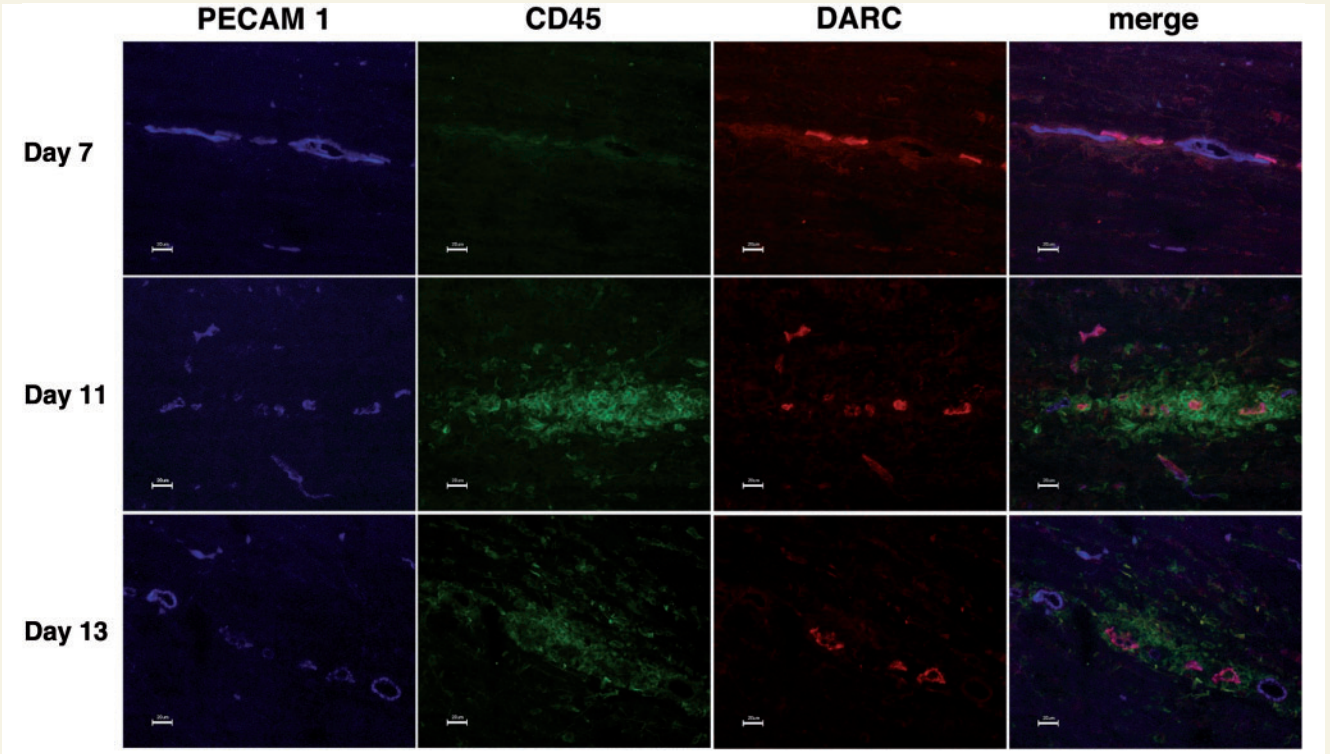

Figure 2 Detection of DARC at the protein level on inflamed CNS vessels. Immunofluorescence staining of frozen spinal cord tissue sections at different time points during EAE pathogenesis of wild-type C57BL/6 mice. Mice were immunized with MOG_{35-55} peptide emulsified in complete Freund's adjuvant and tissues were prepared at Day 7, Day 11 and Day 13 post-immunization. Triple immunofluorescence staining for PECAM1 (blue), CD45 (green) and DARC (red). Specific immunostaining for DARC was detectable at Day 7 after induction of EAE. Scale bar = 20 μm. One experiment out of three analysing three mice per time point is shown.

these controls, quantification showed a comparable collagen IV-positive vessel density in subcortical white matter between controls and patients with multiple sclerosis and identified a higher number of DARC-positive vessels in multiple sclerosis than in control white matter (Fig. 3G). Furthermore, the higher number of DARC-positive vessels detected in multiple sclerosis tissue was equally observed in normal appearing white matter, chronic active lesions and chronic inactive lesions (Fig. 3). Taken together these findings show that DARC is expressed in a subset of brain micovessels in humans. In chronic neuroinflammatory diseases, including multiple sclerosis, a significantly higher number of DARC-positive microvessels could be detected, corresponding to our findings in EAE.

Endothelial DARC shuttles inflammatory chemokines across the blood–brain barrier *in vitro*

A proinflammatory role for endothelial DARC in EAE pathogenesis could be envisaged such that DARC transports chemokines from the abluminal to the luminal side of the blood–brain barrier and thus facilitates leucocyte trafficking across this vascular barrier. As this hypothesis can only be directly tested *in vitro* by studying chemokine transport across brain endothelial cells, we first asked if DARC is expressed in endothelial cells used as *in vitro* blood–brain barrier models such as the brain endothelioma cell line bEnd5 or pMBMECs (Steiner *et al*., 2011). We performed quantitative PCR analysis of total messenger RNA preparations of bEnd5 and of pMBMECs cultured for 6 days and of freshly isolated brain microvessels (Fig. 4A). We found very low but measurable levels of *Darc* messenger RNA in freshly isolated brain microvessels arguing for a low constitutive expression of *Darc* messenger RNA in brain endothelial cells *in vivo*. bEnd5 as well as pMBMECs cultured for 6 days expressed *Darc* messenger RNA and 16 h of TNFα treatment further increased the messenger RNA levels to almost 10-fold, confirming that expression of *Darc* messenger RNA is upregulated in inflamed CNS microvascular endothelial cells. Immunostaining of pMBMECs isolated from wild-type SJL mice and $Darc^{-/-}$ SJL mice as a negative control, confirmed cell surface protein expression of DARC on wild-type pMBMECs after stimulation with TNFα (Fig. 4B), whereas specific immunostaining for DARC could not be observed on non-stimulated pMBMECs (data not shown). Thus, upregulated expression of *Darc* messenger RNA was accompanied by increased cell surface expression of DARC protein on inflamed pMBMECs *in vitro*.

To ensure that lack of DARC in brain endothelial cells does not influence barrier characteristics of brain endothelial cells *per se* and would then lead to increased diffusion of chemokines across the $Darc^{-/-}$ endothelial barrier, we investigated the paracellular permeability for small molecular tracers in the size range of chemokines, namely 3 kDa and 10 kDa dextran, across pMBMECs isolated from wild-type and $Darc^{-/-}$ SJL mice. We found no significant differences in the paracellular permeabilities for 3 kDa

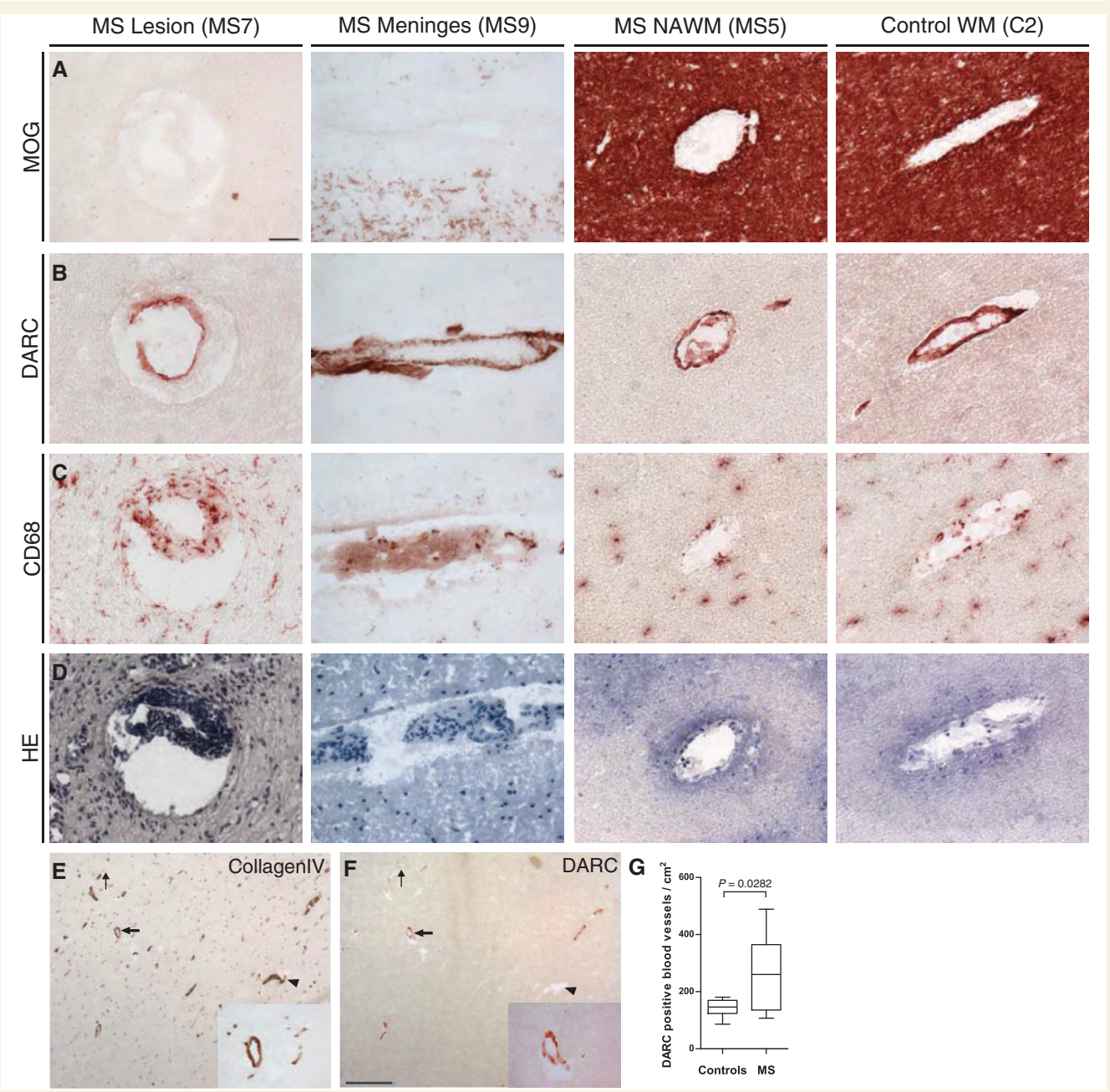

Figure 3 DARC expression in human subcortical white matter of control and multiple sclerosis cases. Immunohistochemical analysis of brain vessels within the human cortex from multiple sclerosis (MS) cases with active inflammatory demyelinating lesion (first column, MS lesions), within meninges (second column, MS Meninges), within normal appearing white matter (third column, MS NAWM) and from a control case within subcortical white matter (fourth column, Control WM) are shown. MOG: MOG immunohistochemistry for myelin differentiating demyelinating lesions from normal myelinated areas in cerebral cortex and subcortical cortical white matter in multiple sclerosis and controls (**A**). DARC: DARC-positive blood vessels were detected in all areas in multiple sclerosis cases and in controls (**B**). CD68: CD68 immunohistochemistry detects inflamed blood vessels (first panel) as well as activated microglia throughout the white matter (**C**). HE: Histology shown by haematoxylin and eosin staining of the corresponding area (**D**). Scale bar = 50 μm. *Bottom*: Collagen IV immunohistochemistry in multiple sclerosis normal appearing white matter identifying all blood vessels (**E**), whereas DARC staining could only be detected in a subset of blood vessels (**F**, arrows). DARC immunoreactivity was detected in larger (large arrow, higher magnification in inset) as well as in smaller blood vessels (small arrow). Insets show area around the blood vessel highlighted by the large arrow. Arrowhead points to a blood vessel, which is DARC-negative. Scale bar = 500 μm. (**G**) Quantification showing more DARC-positive blood vessels in multiple sclerosis normal appearing white matter compared with control white matter (*P*-value = 0.0282).

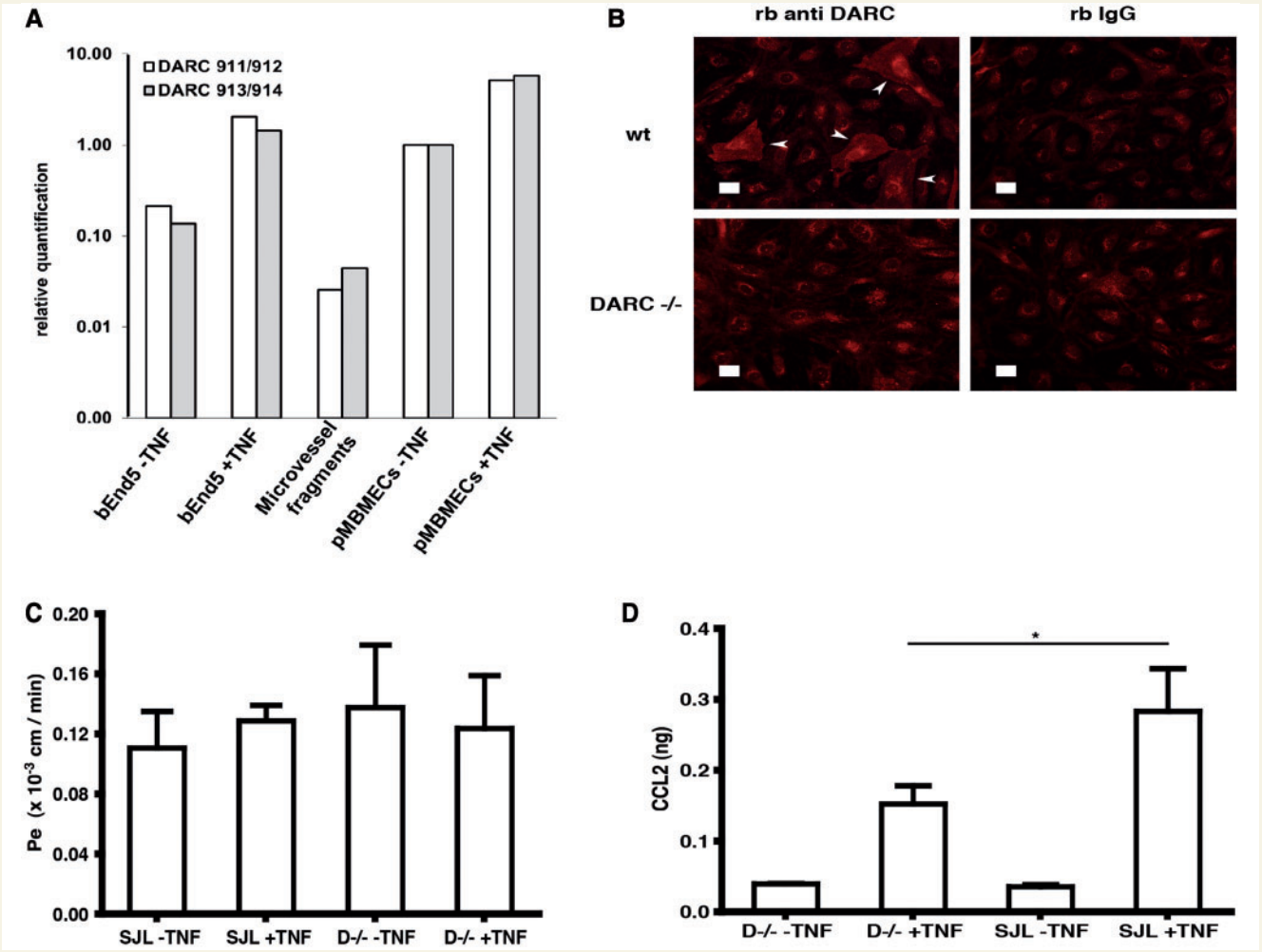

Figure 4 Characterization of *Darc*$^{-/-}$ *in vitro* blood–brain barrier models. (**A**) Quantitative PCR analysis of *Darc* messenger RNA expression in bEnd5, freshly isolated and cultured pMBMECs. bEnd5 and pMBMECs were cultured for 6 days and were either TNFα (16 h) stimulated or not. Freshly isolated brain microvessels were used as a control. Quantitative PCR was performed with two different primer pairs (911/912, 913/914) and *Darc* expression levels are shown relative to that of unstimulated pMBMECs (set to 1.0). Stimulation with TNFα upregulated *Darc* messenger RNA expression in bEnd5 (10-fold) and in pMBMECs (5- to 6-fold). One experiment out of two with comparable results is shown. (**B**) Immunostaining for DARC on pMBMECs. pMBMECs from wild-type SJL (wt; *upper* panel) and *Darc*$^{-/-}$ SJL (DARC −/−; *lower* panel) mice were cultured for 6 days on matrigel-coated permanox chamber slides and were TNFα stimulated 16 h before staining. Positive and specific immunostaining for DARC with the rabbit anti-mouse DARC antibody could only be observed on individual TNFα stimulated pMBMECs from wild-type SJL mice as indicated by white arrowheads (*top left*) despite high background staining observed using rabbit IgG. We did not observe DARC-immunostaining on non-stimulated pMBMECs (data not shown). Scale bars = 20 μm. (**C**) Dextran (10 kDa) permeability across wild-type and DARC-deficient pMBMECs. The permeability coefficients Pe of 10 kDa dextran for unstimulated and stimulated pMBMECs from wild-type (SJL-TNF and SJL + TNF) or DARC-deficient (D−/−-TNF and D−/− + TNF) SJL mice are shown. Bars represent mean ± SEM of three independent experiments. No statistically significant differences of Pe between unstimulated or TNF-α stimulated pMBMECs from *Darc*$^{-/-}$ and wild-type SJL mice were observed. (**D**) CCL2 chemokine secretion of pMBMECs. CCL2 chemokine secretion of DARC-deficient (D−/−) and wild-type (SJL) SJL pMBMECs stimulated (+ TNF) or not (-TNF) with TNFα for 16 h was determined after 3 h by ELISA. The total amount of chemokine found in the upper compartment (150 ml) was calculated and the bars show mean ± SD. A significant difference in CCL2 production between TNF-α stimulated *DARC*$^{-/-}$ and wild-type pMBMECs was found. *$P < 0.05$. One experiment out of three with reproducible results is shown. rb = rabbit.

(data not shown) and 10 kDa (Fig. 4C) dextrans between non-stimulated or TNF-α stimulated pMBMECs isolated from wild-type or *Darc*$^{-/-}$ SJL mice. Thus absence of DARC did not influence barrier integrity of brain endothelial cells *in vitro*.

In addition, brain endothelial cells have been described to express, upon stimulation, inflammatory chemokines such as CCL2. Endogenous chemokine expression could thus impair the analysis of exogenous chemokine transport across the blood–brain barrier *in vitro*. We therefore tested production of the chemokines CCL2 (JE), CCL5 (RANTES) and CXCL1 (KC), which we previously found to be upregulated in inflamed CNS microvessels during EAE (Alt *et al*., 2005) and the homeostatic chemokine CCL21, which does not bind DARC, as a control from wild-type and *Darc*$^{-/-}$ pMBMECs grown on filters and stimulated or not with TNF-α

after a 3 h and 16 h timespan. Analysing the culture supernatants of pMBMBEs by ELISA we did not detect measurable levels of CCL21 and CXCL1 either at 3 h or at 16 h of incubation (data not shown). CCL5 was detected in supernatants of TNF-α stimulated wild-type and *Darc*$^{-/-}$ pMBMECs at 16 h but not at 3 h, reaching a maximal concentration of 0.1 ng/150 μL. In contrast we found that wild-type and *Darc*$^{-/-}$ pMBMECs constitutively produced up to 0.8 ng/150 ml CCL2 within 16 h and up to 2.5 ng/150 μL when previously stimulated with TNF-α. However, within 3 h, the time window required to study exogenous chemokine transport across the blood–brain barrier *in vitro*, CCL2 production remained very low reaching a maximum of 0.3 ng/150 microliters in TNFα stimulated pMBMECs (Fig. 4D). Interestingly, CCL2 production of TNFα stimulated Darc$^{-/-}$ pMBMECs remained significantly lower when compared with TNFα stimulated wild-type pMBMECs. In any case, we felt confident to investigate the transport of exogenously added chemokines across pMBMECs within a timeframe of 3 h *in vitro*.

The inflammatory chemokines CCL2, CCL5 and CXCL1 are potential ligands for DARC, whereas the homeostatic chemokine CCL21 does not bind DARC. We therefore investigated the transport of these chemokines from the abluminal to the luminal compartment across pMBMECs from wild-type and *Darc*$^{-/-}$ SJL mice grown on filter inserts and stimulated or not for 16 h with TNFα. Thirty nanograms of the respective recombinant chemokine was added to the lower compartment of the two chamber transwell assay system and samples from the upper compartment were taken at 1, 2 and 3 h of incubation, frozen immediately and later analysed by ELISA. Transport of CCL21 across pMBMECs was very low and as expected, we found no difference in the transport of CCL21 from the abluminal to the luminal compartment between wild-type and *Darc*$^{-/-}$ pMBMECs (Fig. 5). Transport of CCL21 was also not increased across TNFα stimulated pMBMECs. Although human DARC binds CXCL1 with high affinity (Gardner *et al.*, 2004), transport of murine CXCL1 across

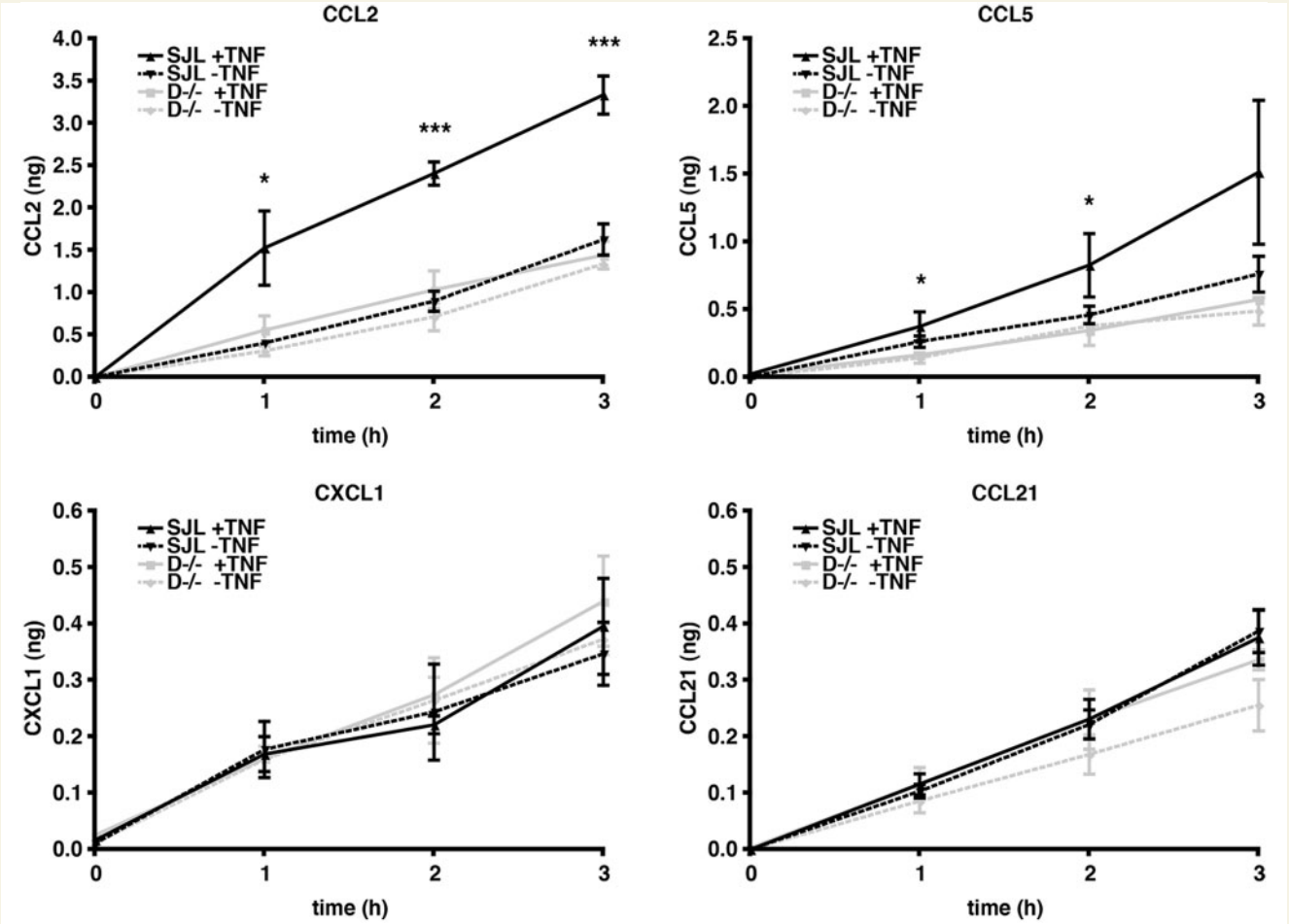

Figure 5 DARC shuttles CCL2 and CCL5 across the inflamed blood–brain barrier *in vitro*. Transport of recombinant chemokines from the basolateral to the luminal side of wild-type SJL pMBMECs (SJL, black lines) or *Darc*$^{-/-}$ SJL pMBMECs (D−/− , grey lines) with (+ TNF) or without (−TNF) TNFα-stimulation is shown. Samples were taken at 1, 2 and 3-h time points and analysed in triplicates by ELISA. ELISA data were analysed using Instat Prism and Microsoft Excel and the total amount of chemokine, which was translocated to the upper compartment, was calculated. Translocation of CCL2 and CCL5 across TNFα stimulated SJL pMBMEC was found to be significantly increased (solid black lines) correlating with induction of DARC expression after TNFα stimulation. CXCL1 and CCL21 were not translocated in a DARC-dependent manner. One out of three independent experiments is shown. Data were analysed using Instat Prism and Microsoft Excel. Line graphs show mean ± SD.

pMBMECs was observed to be equally low as that of CCL21 and was independent of the expression of DARC (Fig. 5). In contrast, transport of CCL5 and CCL2 was generally more efficient and found to be significantly increased across TNF-α stimulated pMBMECs from wild-type SJL mice but not from *Darc*$^{-/-}$ SJL mice when compared to the respective non-stimulated pMBMECs (Fig. 5). As we found expression of DARC to be upregulated on pMBMECs after TNFα stimulation (Fig. 4A), these observations demonstrate an active role for endothelial DARC in mediating the transport of CCL2 and CCL5 but not of CXCL1 from the abluminal to the luminal side of pMBMECS. These data therefore support a pro-inflammatory function of DARC expressed in brain endothelial cells in EAE pathogenesis by shuttling chemokines across the blood–brain barrier.

Darc$^{-/-}$ C57BL/6 and *Darc*$^{-/-}$ SJL mice develop ameliorated experimental autoimmune encephalomyelitis

To investigate the functional contribution of DARC in EAE pathogenesis we next investigated if development of EAE is impaired in the absence of DARC. To this end *Darc*$^{-/-}$ mice were backcrossed into the EAE susceptible mouse stains C57BL/6 and SJL for at least 10 generations and the development of actively induced EAE was compared in *Darc*$^{-/-}$ C57BL/6 and *Darc*$^{-/-}$ SJL mice and the respective C57BL/6 and SJL wild-type littermate control mice. Although we did not observe a significant difference in disease onset, *Darc*$^{-/-}$ C57BL/6 and *Darc*$^{-/-}$ SJL mice developed a milder clinical disease during the first clinical episode of EAE when compared with the respective wild-type control mice (Fig. 6). Furthermore, *Darc*$^{-/-}$ C57BL/6 maintained a milder chronic disease compared to wild-type C57BL/6 mice, and *Darc*$^{-/-}$ SJL mice completely recovered before developing a milder relapse when compared with wild-type SJL mice (Fig. 4). Using the area under the curve as a measure for overall disease activity (Fleming *et al*., 2005), we found a significantly reduced severity of clinical EAE in *Darc*$^{-/-}$ C57BL/6 and *Darc*$^{-/-}$ SJL mice compared with their respective wild-type littermates of the same strain supporting a functional role of DARC in EAE pathogenesis. Immunohistological stainings for CD45^{+} inflammatory infiltrates and for CD3^{+} T cells, B220^{+} B cells, Gr1^{+} and CD11b^{+} myeloid cells in brain and spinal cord sections of wild-type and *Darc*$^{-/-}$ C57BL/6 and SJL mice during the peak of EAE suggested the presence of smaller inflammatory infiltrates in *Darc*$^{-/-}$ SJL and *Darc*$^{-/-}$ C57BL/6 mice when compared with wild-type controls, however, we did not observe striking differences in the number of inflammatory cuffs or their cellular composition (data not shown).

Darc$^{-/-}$ mice C57BL/6 mice have no defect in antigen-specific T cell priming and proliferation

Expression of DARC was previously described on high endothelial venules in peripheral lymph nodes (Kashiwazaki *et al*., 2003). We confirmed specific immunostaining for DARC on high endothelial venules in pheripheral lymph nodes of healthy C57BL/6 and SJL mice using our novel anti-mouse DARC antibody (data not shown). We first asked if expression of DARC is altered in draining lymph nodes after induction of EAE. By performing immunostainings on frozen tissue sections of draining lymph nodes taken from C57BL/6 mice at Days 6, 10 and 14 after subcutaneous immunization with $MOG_{aa35–55}$ in complete Freund's adjuvant we found no difference in high endothelial venule-specific immunostaining for DARC (data not shown). As absence of DARC could influence lymphocyte recirculation through non-inflamed or inflamed lymph nodes, we asked if absence of DARC on the high endothelial venules might influence the priming and proliferation of encephalitogenic T cells after induction of EAE. To this end *Darc*$^{-/-}$ C57BL/6 mice and wild-type C57BL/6 mice were subcutaneously immunized with $MOG_{aa35–55}$/complete Freund's adjuvant and subsequently we performed antigen-recall proliferation assays with lymph node cell suspensions from draining lymph nodes at Days 6 and 9 post-immunization. We observed comparable $MOG_{aa35-55}$ specific T cell proliferation responses in wild-type and *Darc*$^{-/-}$ C57BL/6 mice (Fig. 7) and therefore conclude that priming and proliferation of encephalitogenic T cells is not impaired in the absence of DARC.

DARC regulates increased plasma levels of chemokines during experimental autoimmune encephalomyelitis

In addition to endothelial DARC, availability of inflammatory chemokines within the blood stream can be regulated by erythrocyte DARC. Erythrocyte DARC has been reported to serve as a blood reservoir for inflammatory chemokines but at the same time also as a chemokine sink that buffers increases in plasma chemokine levels. To determine the influence of DARC on the presence of circulating chemokines we asked if the inflammatory chemokines CCL2, CCL5 and CXCL1, which we also investigated for their DARC-mediated transport across the blood–brain barrier, can be detected in the plasma of *Darc*$^{-/-}$ and wild-type C57BL/6 mice during EAE. Using a mouse cytokine array we detected CXCL1 and CCL2 in the plasma of C57BL/6 mice but not of *Darc*$^{-/-}$ C57BL/6 mice at the clinical onset (Day 10 post-immunization) of EAE (Fig. 8A). In contrast, CCL5 was not detected in plasma samples of both *Darc*$^{-/-}$ and wild-type C57BL/6 mice. Soluble ICAM1 was investigated as a marker of inflammation and positive control and was observed at comparable levels in the plasma of *Darc*$^{-/-}$ and wild-type C57BL/6 mice (Fig. 8A). Thus, in the absence of DARC, neuroinflammation is not accompanied by the occurrence of increased levels of inflammatory chemokines in the plasma supporting the notion that DARC serves as a blood reservoir for inflammatory chemokines.

To understand if absence of inflammatory chemokines in the plasma of *Darc*$^{-/-}$ C57BL/6 mice during EAE is because of the lack of vascular or erythrocyte DARC we generated reciprocal bone marrow chimeras by transferring bone marrow cells from *Darc*$^{-/-}$ C57BL/6 mice into lethally irradiated wild-type C57BL/6 mice and vice versa. Eight weeks after recovery, active EAE was induced by subcutaneous immunization with $MOG_{aa35–55}$ in complete Freund's adjuvant and plasma samples were collected, and immediately frozen, from the four groups of mice at different days

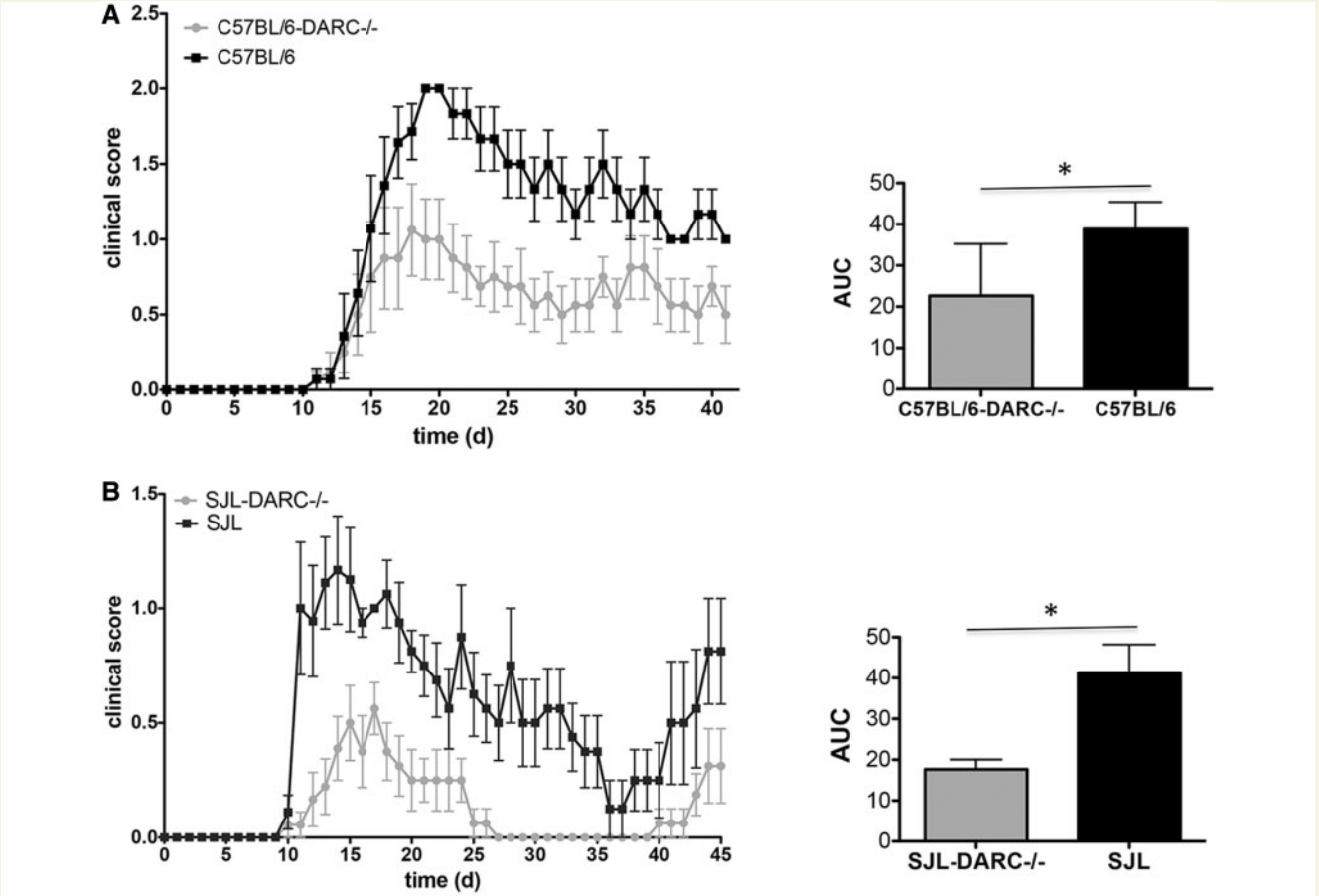

Figure 6 *Darc*$^{-/-}$ SJL or *Darc*$^{-/-}$ C57BL/6 mice develop ameliorated EAE. (**A**) In *Darc*$^{-/-}$ C57BL/6 mice (backcrossing generation N12) and wild-type C57BL/6 littermates active EAE was induced by subcutaneous immunization with $MOG_{aa35–55}$ in complete Freund's adjuvant. The *left* graph shows mean disease scores of 10 animals per group ± SEM, evaluated daily following induction of EAE. (**B**) In *Darc*$^{-/-}$ SJL mice (backcrossing generation N10) active EAE was induced by subcutaneous immunization with $PLP_{139-151}$ in complete Freund's adjuvant. The *left* graph shows mean disease scores of nine animals per group ± SEM, evaluated daily following induction of EAE. The bar graphs show the area under the curve (AUC) calculated from the EAE clinical course for each mouse between Days 0–42 (**A**) or Days 0–45 (**B**) post-immunization. Shown are the mean area under the curve values for each group ± SD. Statistical analysis of area under the curve values with the Mann-Whitney test revealed significantly reduced EAE severity in *Darc*$^{-/-}$ mice (grey bars) compared to wild-type controls (black bars) mice in both C57BL/6 mice (**A**) and SJL mice (**B**). *$P < 0.05$. (**A**) One experiment out of three including a total of 26 *Darc*$^{-/-}$ C57BL/6 and wild-type C57BL/6 mice, respectively is shown. (**B**) One experiment out of three including a total of 24 *Darc*$^{-/-}$ SJL and wild-type SJL mice, respectively is shown.

(Days 6, 10, 14 and 35) post-immunization. In addition we collected plasma samples from non-immunized mice to determine the chemokine plasma concentrations of healthy bone marrow chimeric mice. All plasma samples were tested for CCL2, CCL5 and CXCL1. CCL5 could not be detected in any of the plasma samples investigated. In contrast, very low levels of CCL2 (<50 pg/ml) and low levels of CXCL1 (<500 pg/ml) were already detected in plasma samples in all four groups of non-immunized mice, probably because of the higher sensitivity of the ELISA when compared with the cytokine microarray performed previously (Fig. 8B). After induction of EAE we found significantly increased plasma levels of CXCL1 in both groups of bone marrow chimeric mice expressing DARC on erythrocytes but not in bone marrow chimeric mice lacking erythrocyte DARC, which underscores a role for erythrocyte DARC as a blood reservoir for CXCL1. Increased levels of CXCL1 were detectable on Day 6 post-immunization, before the onset of EAE, and remained elevated on Day 10 post-immunization, coinciding with the onset of clinical EAE. At Day 14 post-immunization, plasma levels of CXCL1 declined to baseline levels (Fig. 8B).

CCL2 plasma concentrations detected in non-immunized bone marrow chimeric mice were 10-fold lower when compared with CXCL1. After induction of EAE, plasma concentrations of CCL2 slightly increased in a similar kinetic in all four groups of chimeric mice reaching significantly increased levels of CCL2 when compared with non-immunized mice at the onset of EAE (Day 10 post-immunization), decreasing to baseline levels at Day 14 post-immunization, and remaining low until Day 35 post-immunization during chronic EAE. At none of the time points investigated did plasma levels of CCL2 significantly differ between the four groups of bone marrow chimeric mice (Fig. 8B) suggesting that plasma levels of CCL2 do not critically rely on the expression of DARC.

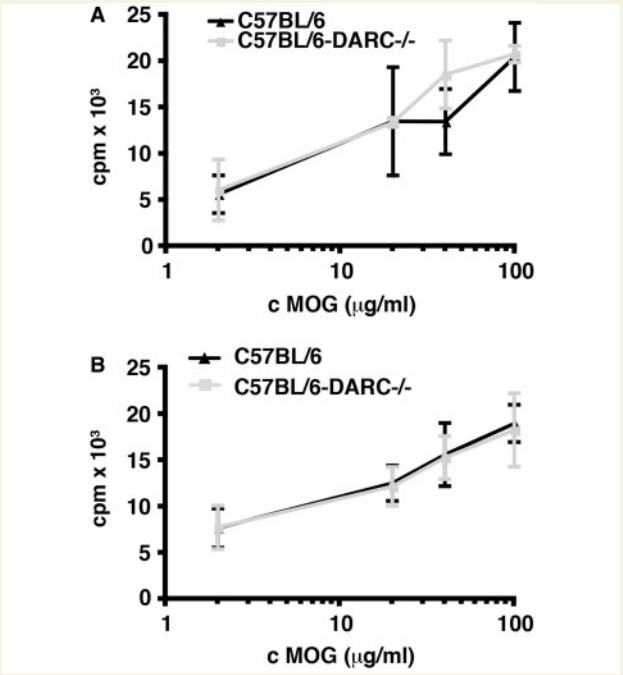

Figure 7 Lack of DARC does not alter antigen-induced T cell proliferation in C57BL/6 mice. Plots show $MOG_{aa35–55}$ peptide induced T cell proliferation of primary cultures from draining lymph node lymphocytes prepared 6 days (**A**) and 9 days (**B**) post-immunization of *Darc*$^{-/-}$ C57BL/6 mice and wild-type C57BL/6 mice upon stimulation with increasing $MOG_{aa35–55}$ peptide concentrations (mean ± SD). MOG-specific proliferation was normalized against baseline proliferation. Proliferation was measured by ^{3}H-dT incorporation. One representative experiment out of six is shown.

Absence of endothelial DARC ameliorates experimental autoimmune encephalomyelitis

Having established apparently opposing roles of endothelial and erythrocyte DARC with vascular DARC shuttling CCL2 but not CXCL1 across the blood–brain barrier and erythrocyte DARC maintaining increased plasma levels of CXCL1 but not of CCL2, we finally asked if ameliorated EAE is due to the lack of endothelial or erythrocyte DARC. To distinguish between a role of erythrocyte and endothelial DARC to EAE pathogenesis, we generated reciprocal bone marrow chimeras by transferring bone marrow cells from *Darc*$^{-/-}$ C57BL/6 mice into lethally irradiated wild-type C57BL/6 mice and vice versa. After a recovery for 8 weeks, active EAE was induced in bone-marrow chimeric mice by subcutaneous immunization with $MOG_{aa35–55}$ in complete Freund's adjuvant. *Darc*$^{-/-}$ C57BL/6 mice, reconstituted with either *Darc*$^{-/-}$ or wild-type C57BL/6 bone marrow cells, showed a delayed onset of EAE when compared with wild-type C57BL/6 mice reconstituted with either *Darc*$^{-/-}$ or wild-type C57BL/6 bone marrow cells (Fig. 9A) and an ameliorated disease as determined by the area under the curve (Fig. 9B). These observations supported our previous observations of ameliorated EAE in *Darc*$^{-/-}$ C57BL/6 mice compared with wild-type C57BL/6 mice

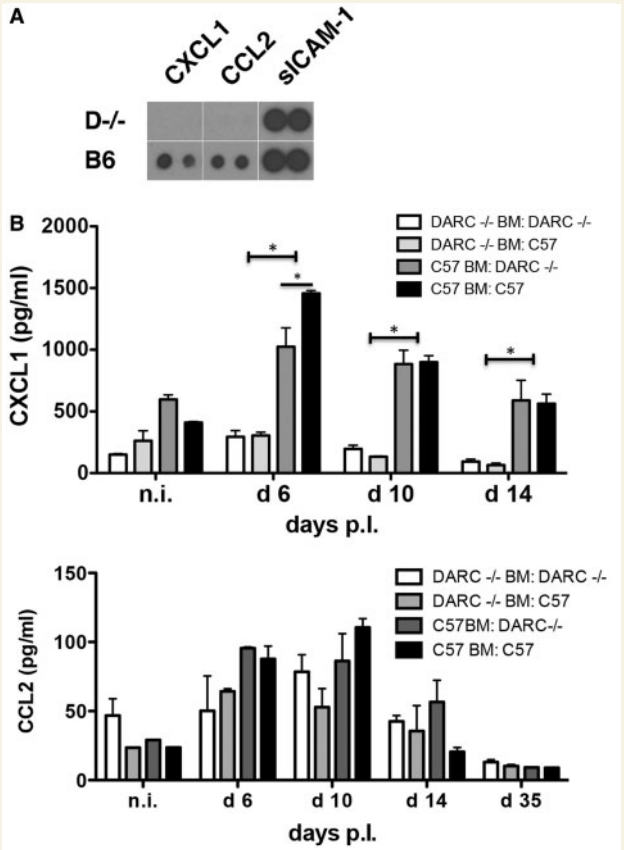

Figure 8 DARC regulates increased plasma levels of chemokines during EAE. (**A**) Mouse cytokine array analysing plasma samples prepared from *Darc*$^{-/-}$ C57BL/6 and wild-type C57BL/6 mice 10 days post-immunization (p.l.) with $MOG_{aa35–55}$ in complete Freund's adjuvant. CCL2 and CXCL1 were found in the plasma of wild-type C57BL/6 mice but were absent in the plasma of *Darc*$^{-/-}$ C57BL/6 mice. Soluble ICAM1 was chosen as a DARC-independent positive control and detected with comparable signal intensities in both *Darc*$^{-/-}$ C57BL/6 mice and wild-type C57BL/6 controls. One out of two independent experiments is shown. (**B**) CXCL1 (*top*) and CCL2 (*bottom*) plasma levels of bone marrow chimeric mice at different time points during EAE pathogenesis measured by ELISA are shown. White bar = *Darc*$^{-/-}$ BM:*Darc*$^{-/-}$ (*Darc*$^{-/-}$ C57BL/6 mice reconstituted with *Darc*$^{-/-}$ bone marrow); light grey bar = *Darc*$^{-/-}$ BM:C57 (C57BL/6 mice reconstituted with *Darc*$^{-/-}$ bone marrow), dark grey bar = C57 BM: *Darc*$^{-/-}$ (*Darc*$^{-/-}$ C57BL/6 mice reconstituted with C57BL/6 bone marrow), black bar = C57 BM: C57 (C57BL/6 mice reconstituted with C57BL/6 bone marrow). Bars show mean ± SD. Number of samples for CXCL1: non-immunized mice (n.i.) and Day 6 post-immunization $n = 4$; Days 10 and 14 post-immunization $n = 6$. Number of samples for CCL2: $n = 4$ for all timepoints. *Bordered line $P < 0.05$ between both groups of wild-type and *Darc*$^{-/-}$ BM recipients; *simple line $P < 0.05$ between the individual columns. Significantly elevated plasma levels of CXCL1 were only detected in the presence of erythrocyte DARC starting at Day 6 post-immunization before onset of clinical EAE.

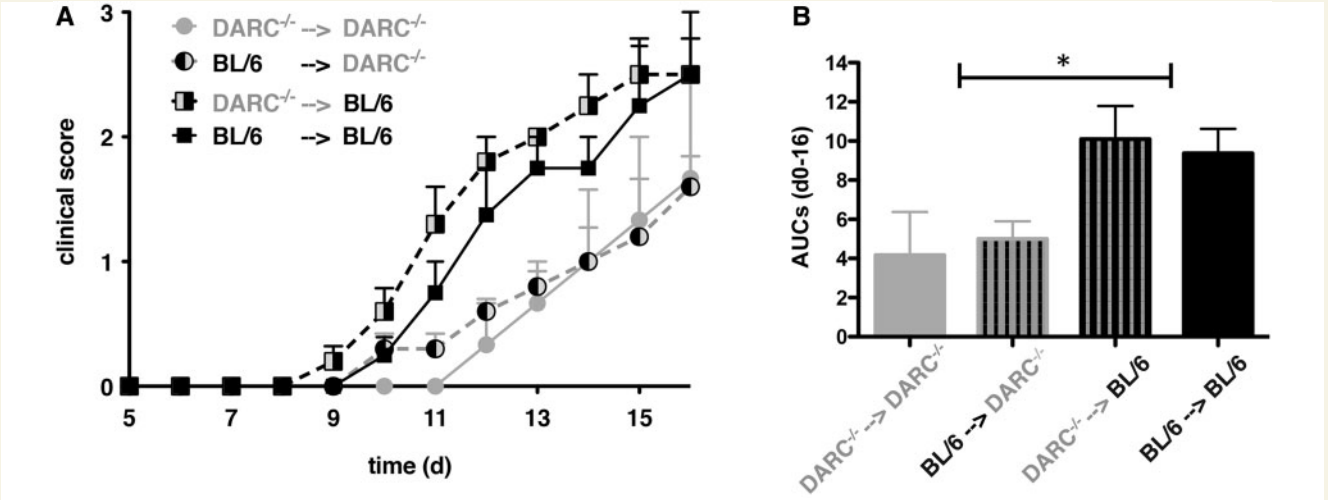

Figure 9 Lack of vascular DARC ameliorates EAE. $MOG_{35–55}$ peptide-induced active EAE in bone marrow chimeric mice (backcrossing generations N11 to N14) is shown. (**A**) The graph shows mean disease scores of five animals per group ± SEM, evaluated daily following induction of EAE. *Darc*$^{-/-}$ C57BL/6 mice reconstituted with *Darc*$^{-/-}$ bone marrow (*DARC*$^{-/-}$ → *DARC*$^{-/-}$; grey filled circles) or C57BL/6 wild-type bone marrow (BL/6 → *DARC*$^{-/-}$; black grey semi-filled circles) developed ameliorated EAE when compared to C57BL/6 mice reconstituted with either C57BL/6 bone marrow (BL6 → BL6; black filled squares) or *Darc*$^{-/-}$ bone marrow (*DARC*$^{-/-}$ → BL/6; grey/black semi-filled squares). (**B**) Area under the curve (Days 0–16 post-immunization) as a measure for overall disease severity was calculated and found to be significantly reduced (*$P < 0.05$) in *Darc*$^{-/-}$ C57BL/6 mice reconstituted with either wild-type or *Darc*$^{-/-}$ bone marrow, when compared to wild-type recipients irrespective of reconstitution with wild-type or *Darc*$^{-/-}$ bone marrow. One experiment out of three investigating a total of 10 to 14 mice for each group is shown.

(Fig. 6) and demonstrated that absence of endothelial but not erythrocyte DARC is required for establishing ameliorated EAE (Fig. 9). These observations underscore the pro-inflammatory role of DARC by shuttling chemokines across the blood–brain barrier.

Discussion

DARC belongs to the family of atypical 'silent' chemokine chemokine receptors, which are structurally similar to other G-protein coupled receptors with seven transmembrane spanning helices and extracellular domains binding chemokines with high affinity. In contrast with other chemokine receptors, atypical chemokine receptors including DARC fail to engage G-proteins and therefore do not couple to signalling cascades inducing integrin activation and cell motility. The inability to trigger conventional chemokine responses has led to concepts of chemokine scavenging, sequestration, buffering and transcellular transport by these atypical chemokine receptors. It has been shown that human DARC can bind many, but not all pro-inflammatory CC and CXC chemokines (Gardner *et al*., 2004). Depending on its cellular expression, the biological functions assigned to DARC have been quite different. Whereas erythrocyte DARC was shown to bind chemokines and either serve as a sink or a reservoir for inflammatory chemokines in the circulation, endothelial DARC was described to internalize and transcytose chemokines from their parenchymal sites of synthesis to the luminal side of the endothelium, where the chemokines were found immobilized and could contribute to leucocyte extravasation *in vivo* (Novitzky-Basso and Rot, 2012).

Based on these findings we considered DARC to be a candidate molecule mediating during neuroinflammation the transport of CNS-derived inflammatory chemokines across the highly specialized and polarized endothelial cells forming the blood–brain barrier. Our present study demonstrates that DARC is upregulated on endothelial cells in CNS microvessels during EAE and in multiple sclerosis and contributes to EAE pathogenesis. Although erythrocyte DARC served as a chemokine reservoir during EAE, brain endothelial DARC was found to shuttle recombinant chemokines from the abluminal to the luminal side of an *in vitro* blood–brain barrier model. Absence of endothelial, but not erythrocyte DARC, was responsible for amelioration of EAE in line with a contribution of endothelial DARC in shuttling inflammatory chemokines from the CNS parenchyma across the blood–brain barrier influencing immune cell interaction with the inflamed blood–brain barrier during EAE and multiple sclerosis.

The infiltration of immune cells into the CNS is an essential step in the neuropathogenesis of multiple sclerosis and its animal model EAE. Live cell imaging studies observing the interaction of encephalitogenic T cells with brain or spinal cord microvessels during EAE demonstrated the prerequisite of G-protein coupled receptor signalling for the integrin-mediated firm arrest of T cells to the inflamed CNS microvessels (Vajkoczy *et al*., 2001; Piccio *et al*., 2002). These observations suggested the involvement of chemokines available on the luminal surface of the blood–brain barrier endothelium in T cell trafficking across the blood–brain barrier. Glycosaminoglycans (GAGs), most importantly heparan

sulphates, are abundant on the luminal surface of endothelial cells including brain endothelial cells, and have been shown to avidly bind chemokines (Parish, 2006). Luminal presence of CCL2 and CCL5 on the blood–brain barrier has been suggested by live cell imaging studies demonstrating that antibodies blocking CCL2 and CCL5 prevented leucocyte adhesion but not rolling in the inflamed brain microvasculature during EAE (dos Santos *et al*., 2005).

Interestingly, although expression of CCL2 and CCL5 can readily be detected in cultured brain endothelial cells *in vitro* (Holman *et al*., 2011), in multiple sclerosis lesions and in EAE, both chemokines are expressed rather by astrocytes or infiltrating immune cells (Ubogu *et al*., 2006). In contrast, expression of the homeostatic chemokines CCL19 and CCL21 was found to be upregulated in brain endothelial cells in a mouse model of EAE (Alt *et al*., 2002) and in multiple sclerosis lesions (Krumbholz *et al*., 2007), but their involvement in leucocyte migration across the blood–brain barrier during neuroinflammation remains to be shown. In addition, increased CNS expression of CXCL12 in EAE and multiple sclerosis was found to be accompanied by the loss of polarized expression of this chemokine in CNS microvascular endothelial cells (McCandless *et al*., 2006, 2008). CXCL12 might therefore become luminally available during neuroinflammation and mediate T cell arrest to the inflamed blood–brain barrier in EAE and multiple sclerosis (McCandless *et al*., 2006, 2008; Moll *et al*., 2009).

In addition to homeostatic chemokines, there is abundant evidence for the involvement of inflammatory chemokines and their receptors e.g. CCR1 (Rottman *et al*., 2000), CCR2 (Fife *et al*., 2000; Izikson *et al*., 2000) and CXCR2 (Carlson *et al*., 2008), in the pathogenesis of EAE and multiple sclerosis (Ubogu *et al*., 2006). Intriguingly, most of the chemokines shown to be involved in EAE pathogenesis are expressed by glial cells or inflammatory cells localized in the CNS parenchyma in EAE brains and multiple sclerosis lesions (Glabinski *et al*., 1998; Sorensen *et al*., 1999; Lund *et al*., 2004; Omari *et al*., 2006). Considering the unique barrier characteristics of the brain endothelial cells it is highly unlikely that sufficient amounts of these chemokines diffuse across the blood–brain barrier to target circulating immune cells into the CNS. Thus, the contribution of inflammatory chemokines to the pathogenesis of multiple sclerosis and EAE by mediating the migration of circulating leucocytes across the blood–brain barrier into the CNS requires the existence of a putative transport mechanism for inflammatory chemokines from the abluminal to the luminal side of the blood–brain barrier endothelium.

In fact it has been demonstrated that CCL2 can be transported from the abluminal to the luminal side of brain microvascular endothelial cells by a transcellular mechanism that at least in part involves binding of CCL2 to CCR2 and caveolae (Dzenko *et al*., 2001; Ge *et al*., 2008).

Another potential candidate molecule able to transport chemokines across the blood–brain barrier is the atypical chemokine receptor DARC, which binds most inflammatory chemokines. DARC is expressed in microvascular endothelial cells in peripheral organs and the current view is that DARC can mediate the transcellular transport of chemokines across vascular barriers. Support for this view came from elegant *in situ* studies that followed the trafficking of radiolabelled chemokines in skin explants from the interstitial space through the vesicular network of endothelial cells to the luminal surface of venules where they co-localized with DARC immunoreactivity (Middleton *et al*., 1997; Hub and Rot, 1998; Pruenster *et al*., 2009). In heterologous transfectants DARC was shown to relocalize from the basolateral to the apical side through an intracellular vesicular compartment upon binding of inflammatory chemokines (Pruenster *et al*., 2009). In this study it was also shown that the functional chemokines translocated with DARC. The precise mechanism of DARC-mediated chemokine transcytosis remains to be investigated. Although some studies localized DARC to caveolin 1 and therefore to caveolae as vesicular transport compartment (Luo *et al*., 1997; Middleton *et al*., 1997) DARC-mediated chemokine endocytosis seems to occur through a macropinocytosis-like process in endothelial cells for which caveolin 1 was dispensable (Zhao *et al*., 2011).

These findings prompted us to investigate if DARC is also expressed at the blood–brain barrier and could serve as a chemokine shuttle across the blood–brain barrier during neuroinflammation. In a gene expression profiling study we identified upregulated expression of DARC in cerebral microvessel preparations from C57BL/6 and SJL mice suffering from EAE compared with microvessel preparations of healthy control mice (Alt *et al*., 2005). A similar approach confirmed upregulated expression of DARC in acute white matter lesions in the brain of a patient with multiple sclerosis, when compared with normal-appearing white matter (Whitney *et al*., 1999). Performing *in situ* hybridization and immunohistology in the present study we demonstrate increased expression and immunostaining of DARC in CNS microvessels starting before the clinical onset of EAE. As most of the inflammatory chemokines involved in EAE pathogenesis are upregulated in the CNS during preclinical stages already (Carlson *et al*., 2008) this finding further supports a potential involvement of endothelial DARC in shuttling inflammatory chemokines from the CNS parenchyma to the luminal surface of the blood–brain barrier. Detection of increased DARC immunostaining in brain microvessels in acute lesions of multiple sclerosis brains further corroborates the contribution of DARC to autoimmune neuroinflammation. Using a well-differentiated mouse *in vitro* blood–brain barrier model that has proven to reliably mimic blood–brain barrier characteristics under physiological and pathological conditions (Coisne *et al*., 2005, 2013; Enzmann *et al*., 2013), we found that expression of DARC in brain endothelial cells is upregulated by proinflammatory stimuli and that expression of endothelial DARC correlates with increased basolateral to luminal transport of recombinant CCL2 and CCL5 but not of CXCL1 *in vitro*. As to date there are no binding studies investigating the interaction of mouse DARC with mouse chemokines, the affinity of CXCL1 to murine DARC is unknown. In contrast, human DARC has been shown to bind CCL2, CCL5 and CXCL1 with similarly high affinities (Gardner *et al*., 2004). As we used recombinant chemokines in this assay, which might be different from endogenous chemokines in their post-translational modifications including but not limited to their glycosylation patterns, one could speculate that post-translational modification of recombinant CXCL1 might not be favourable for DARC binding. Finally, our *in vitro* studies investigating DARC-mediated chemokine shuttling across the blood–brain barrier have employed recombinant chemokines,

It is noteworthy, however, that the amounts of CXCL1 we found to be shuttled across the tight brain endothelial cell monolayers *in vitro* independent of DARC expression were in general 5- to 10-fold below those detected for CCL5 and CCL2, respectively.

In contrast, when studying the role of erythrocyte DARC during EAE in reciprocal bone marrow chimeras we found plasma levels of soluble endogenous CXCL1 but less so of CCL2 to strictly depend on erythrocyte but not on endothelial DARC. This could be due to a different glycosylation status of the respective chemokines within the circulation versus the inflamed CNS parenchyma, which might differentially influence chemokine binding to endothelial versus erythrocyte DARC. In any case, these findings confirm the function of erythrocyte DARC as a chemokine reservoir rather than a chemokine sink also in neuroinflammation. Plasma levels of CCL2 were found be 10-fold lower than those detected for CXCL1, which might be an alternative explanation of the lack of a significant correlation of increased CCL2 plasma levels with erythrocyte DARC in EAE.

In contrast, increased plasma levels of CXCL1 were detected in bone marrow chimeric mice expressing erythrocyte DARC before the onset of the clinical disease 6 days after the induction of EAE. As CXCL1 can be induced by IL17 it is tempting to speculate that in contrast to CCL2, CXCL1 might be induced by encephalitogenic T_{H17} cells in peripheral tissues and thus might readily be detected in the plasma of mice expressing erythrocyte DARC (Onishi and Gaffen, 2010).

Involvement of DARC in EAE pathogenesis is demonstrated by our findings that absence of DARC ameliorates chronic EAE in C57BL/6 mice and relapsing-remitting EAE in SJL/ mice. When addressing the impact of erythrocyte DARC versus endothelial DARC in EAE pathogenesis using reciprocal bone marrow chimeric mice, we found that absence of endothelial rather than erythrocyte DARC ameliorated the disease course. Although our findings confirmed an important role of erythrocyte DARC as a chemokine reservoir in the blood stream during EAE, this function of DARC seems to have no significant influence in EAE pathogenesis. In contrast, endothelial DARC contributes to EAE pathogenesis by shuttling chemokines across the blood–brain barrier.

In summary our study demonstrates the involvement of endothelial DARC in mediating the transport of inflammatory chemokines across the blood–brain barrier during neuroinflammation and its impact in disease severity and progression.

Funding

For this study the BE laboratory has been supported by the Kamillo-Eisner Foundation, the Swiss Multiple Sclerosis Society, the Swiss National Science Foundation (grant N° 31003A_118390) and the Microscopy Imaging Center of the University of Bern (www.mic.unibe.ch). AR laboratory has been supported by MRC Grants G0802838 to AR and G9818340 to MRC CIR; the NSW laboratory has been supported by the National Multiple Sclerosis Society (grant RG 4249A2/2).

Supplementary material

Supplementary material is available at *Brain* online.

References

Alt C, Duvefelt K, Franzén B, Yang Y, Engelhardt B. Gene and protein expression profiling of the microvascular compartment in experimental autoimmune encephalomyelitis in C57Bl/6 and SJL mice. Brain Pathol 2005; 15: 1–16.

Alt C, Laschinger M, Engelhardt B. Functional expression of the lymphoid chemokines CCL19 (ELC) and CCL 21 (SLC) at the blood-brain barrier suggests their involvement in G-protein-dependent lymphocyte recruitment into the central nervous system during experimental autoimmune encephalomyelitis. Eur J Immunol 2002; 32: 2133–44.

Carlson T, Kroenke M, Rao P, Lane TE, Segal B. The Th17-ELR+ CXC chemokine pathway is essential for the development of central nervous system autoimmune disease. J Exp Med 2008; 205: 811–23.

Coisne C, Dehouck L, Faveeuw C, Delplace Y, Miller F, Landry C, et al. Mouse syngenic *in vitro* blood-brain barrier model: a new tool to examine inflammatory events in cerebral endothelium. Lab Invest 2005; 85: 734–46.

Coisne C, Lyck R, Engelhardt B. Live cell imaging techniques to study T cell trafficking across the blood-brain barrier *in vitro* and *in vivo*. Fluids Barriers CNS 2013; 10: 7.

Dawson TC, Lentsch AB, Wang Z, Cowhig JE, Rot A, Maeda N, et al. Exaggerated response to endotoxin in mice lacking the Duffy antigen/receptor for chemokines (DARC). Blood 2000; 96: 1681–4.

Doring A, Wild M, Vestweber D, Deutsch U, Engelhardt B. E- and P-selectin are not required for the development of experimental autoimmune encephalomyelitis in C57BL/6 and SJL Mice. J Immunol 2007; 179: 8470–9.

dos Santos AC, Barsante MM, Arantes RM, Bernard CC, Teixeira MM, Carvalho-Tavares J. CCL2 and CCL5 mediate leukocyte adhesion in experimental autoimmune encephalomyelitis—an intravital microscopy study. J Neuroimmunol 2005; 162: 122–9.

Dzenko KA, Andjelkovic AV, Kuziel WA, Pachter JS. The chemokine receptor CCR2 mediates the binding and internalization of monocyte chemoattractant protein-1 along brain microvessels. J Neurosci 2001; 21: 9214–23.

Engelhardt B, Kappos L. Natalizumab: targeting alpha4-integrins in multiple sclerosis. Neurodegener Dis 2008; 5: 16–22.

Engelhardt B, Kempe B, Merfeld-clauss S, Laschinger M, Furie B, Wild MK, et al. P-selectin glycoprotein ligand 1 is not required for the development of experimental autoimmune encephalomyelitis in SJL and C57BL/6 mice. J Immunol 2005; 175: 1267–75.

Engelhardt B, Laschinger M, Schulz M, Samulowitz U, Vestweber D, Hoch G. The development of experimental autoimmune encephalomyelitis in the mouse requires alpha4-integrin but not alpha4beta7-integrin. J Clin Invest 1998; 102: 2096–105.

Engelhardt B, Ransohoff RM. Capture, crawl, cross: the T cell code to breach the blood-brain barriers. Trends Immunol 2012; 33: 579–89.

Engelhardt B, Sorokin L. The blood-brain and the blood-cerebrospinal fluid barriers: function and dysfunction. Semin Immunopathol 2009; 31: 497–511.

Enzmann G, Mysiorek C, Gorina R, Cheng YJ, Ghavampour S, Hannocks MJ, et al. The neurovascular unit as a selective barrier to polymorphonuclear granulocyte (PMN) infiltration into the brain after ischemic injury. Acta Neuropathol 2013; 125: 395–412.

Fife BT, Huffnagle GB, Kuziel WA, Karpus WJ. CC chemokine receptor 2 is critical for induction of experimental autoimmune encephalomyelitis. J Exp Med 2000; 192: 899–905.

Fleming KK, Bovaird JA, Mosier MC, Emerson MR, Levine SM, Marquis JG. Statistical analysis of data from studies on experimental autoimmune encephalomyelitis. J Neuroimmunol 2005; 170: 71–84.

Gardner L, Patterson AM, Ashton BA, Stone MA, Middleton J. The human Duffy antigen binds selected inflammatory but not homeostatic chemokines. Biochem Biophys Res Commun 2004; 321: 306–12.

Ge S, Song L, Serwanski DR, Kuziel WA, Pachter JS. Transcellular transport of CCL2 across brain microvascular endothelial cells. J Neurochem 2008; 104: 1219–32.

Glabinski AR, Krakowski M, Han Y, Owens T, Ransohoff RM. Chemokine expression in GKO mice (lacking interferon-gamma) with experimental autoimmune encephalomyelitis. J Neurovirol 1999; 5: 95–101.

Glabinski AR, Tuohy VK, Ransohoff RM. Expression of chemokines RANTES, MIP-1alpha and GRO-alpha correlates with inflammation in acute experimental autoimmune encephalomyelitis. Neuroimmunomodulation 1998; 5: 166–71.

Holman DW, Klein RS, Ransohoff RM. The blood-brain barrier, chemokines and multiple sclerosis. Biochim Biophys Acta 2011; 1812: 220–30.

Horuk R, Martin A, Hesselgesser J, Hadley T, Lu ZH, Wang ZX, et al. The Duffy antigen receptor for chemokines: structural analysis and expression in the brain. J Leukoc Biol 1996; 59: 29–38.

Hub E, Rot A. Binding of RANTES, MCP-1, MCP-3, and MIP-1alpha to cells in human skin. Am J Pathol 1998; 152: 749–57.

Izikson L, Klein RS, Charo IF, Weiner HL, Luster AD. Resistance to experimental autoimmune encephalomyelitis in mice lacking the CC chemokine receptor (CCR)2. J Exp Med 2000; 192: 1075–80.

Kashiwazaki M, Tanaka T, Kanda H, Ebisuno Y, Izawa D, Fukuma N, et al. A high endothelial venule-expressing promiscuous chemokine receptor DARC can bind inflammatory, but not lymphoid, chemokines and is dispensable for lymphocyte homing under physiological conditions. Int Immunol 2003; 15: 1219–27.

Krumbholz M, Theil D, Steinmeyer F, Cepok S, Hemmer B, Hofbauer M, et al. CCL19 is constitutively expressed in the CNS, up-regulated in neuroinflammation, active and also inactive multiple sclerosis lesions. J Neuroimmunol 2007; 190: 72–9.

Lee JS, Frevert CW, Thorning DR, Segerer S, Alpers CE, Cartron JP, et al. Enhanced expression of Duffy antigen in the lungs during suppurative pneumonia. J Histochem Cytochem 2003; 51: 159–66.

Lennon G, Auffray C, Polymeropoulos M, Soares MB. The I.M.A.G.E. Consortium: an integrated molecular analysis of genomes and their expression. Genomics 1996; 33: 151–2.

Lund BT, Ashikian N, Ta HQ, Chakryan Y, Manoukian K, Groshen S, et al. Increased CXCL8 (IL-8) expression in Multiple Sclerosis. J Neuroimmunol 2004; 155: 161–71.

Luo H, Chaudhuri A, Johnson KR, Neote K, Zbrzezna V, He Y, et al. Cloning, characterization, and mapping of a murine promiscuous chemokine receptor gene: homolog of the human Duffy gene. Genome Res 1997; 7: 932–41.

Lyck R, Ruderisch N, Moll AG, Steiner O, Cohen CD, Engelhardt B, et al. Culture-induced changes in blood-brain barrier transcriptome: implications for amino-acid transporters *in vivo*. J Cereb Blood Flow Metab 2009; 29: 1491–502.

Mccandless EE, Piccio L, Woerner BM, Schmidt RE, Rubin JB, Cross AH, et al. Pathological expression of CXCL12 at the blood-brain barrier correlates with severity of multiple sclerosis. Am J Pathol 2008; 172: 799–808.

Mccandless EE, Wang Q, Woerner BM, Harper JM, Klein RS. CXCL12 limits inflammation by localizing mononuclear infiltrates to the perivascular space during experimental autoimmune encephalomyelitis. J Immunol 2006; 177: 8053–64.

Middleton J, Neil S, Wintle J, Clark-lewis I, Moore H, Lam C, et al. Transcytosis and surface presentation of IL-8 by venular endothelial cells. Cell 1997; 91: 385–95.

Middleton J, Patterson AM, Gardner L, Schmutz C, Ashton BA. Leukocyte extravasation: chemokine transport and presentation by the endothelium. Blood 2002; 100: 3853–60.

Miyagishi R, Kikuchi S, Takayama C, Inoue Y, Tashiro K. Identification of cell types producing RANTES, MIP-1 alpha and MIP-1 beta in rat experimental autoimmune encephalomyelitis by in situ hybridization. J Neuroimmunol 1997; 77: 17–26.

Moll NM, Cossoy MB, Fisher E, Staugaitis SM, Tucky BH, Rietsch AM, et al. Imaging correlates of leukocyte accumulation and CXCR4/CXCL12 in multiple sclerosis. Arch Neurol 2009; 66: 44–53.

Novitzky-basso I, Rot A. Duffy antigen receptor for chemokines and its involvement in patterning and control of inflammatory chemokines. Front Immunol 2012; 3: 266.

Omari KM, John G, Lango R, Raine CS. Role for CXCR2 and CXCL1 on glia in multiple sclerosis. Glia 2006; 53: 24–31.

Onishi RM, Gaffen SL. Interleukin-17 and its target genes: mechanisms of interleukin-17 function in disease. Immunology 2010; 129: 311–21.

Parish CR. The role of heparan sulphate in inflammation. Nat Rev Immunol 2006; 6: 633–43.

Pfeiffer F, Kumar V, Butz S, Vestweber D, Imhof BA, stein JV, et al. Distinct molecular composition of blood and lymphatic vascular endothelial cell junctions establishes specific functional barriers within the peripheral lymph node. Eur J Immunol 2008; 38: 2142–55.

Pfeiffer F, Schafer J, Lyck R, Makrides V, Brunner S, Schaerenwiemers N, et al. Claudin-1 induced sealing of blood-brain barrier tight junctions ameliorates chronic experimental autoimmune encephalomyelitis. Acta Neuropathol 2011; 122: 601–14.

Piccio L, Rossi B, Scarpini E, Laudanna C, Giagulli C, Issekutz AC, et al. Molecular mechanisms involved in lymphocyte recruitment in inflamed brain microvessels: critical roles for P-selectin glycoprotein ligand-1 and heterotrimeric G(i)-linked receptors. J Immunol 2002; 168: 1940–9.

Pruenster M, Mudde L, Bombosi P, Dimitrova S, Zsak M, Middleton J, et al. The Duffy antigen receptor for chemokines transports chemokines and supports their promigratory activity. Nat Immunol 2009; 10: 101–8.

Ransohoff RM, Hamilton TA, Tani M, Stoler MH, Shick HE, Major JA, et al. Astrocyte expression of mRNA encoding cytokines IP-10 and JE/MCP-1 in experimental autoimmune encephalomyelitis. FASEB J 1993; 7: 592–600.

Rottman JB, Slavin AJ, Silva R, Weiner HL, Gerard CG, Hancock WW. Leukocyte recruitment during onset of experimental allergic encephalomyelitis is CCR1 dependent. Eur J Immunol 2000; 30: 2372–7.

Roy M, Richard JF, Dumas A, Vallieres L. CXCL1 can be regulated by IL-6 and promotes granulocyte adhesion to brain capillaries during bacterial toxin exposure and encephalomyelitis. J Neuroinflammation 2012; 9: 18.

Sorensen TL, Tani M, Jensen J, Pierce V, lucchinetti C, Folcik VA, et al. Expression of specific chemokines and chemokine receptors in the central nervous system of multiple sclerosis patients. J Clin Invest 1999; 103: 807–15.

Steiner O, Coisne C, Cecchelli R, Boscacci R, Deutsch U, Engelhardt B, et al. Differential roles for endothelial ICAM-1, ICAM-2, and VCAM-1 in shear-resistant T cell arrest, polarization, and directed crawling on blood-brain barrier endothelium. J Immunol 2010; 185: 4846–55.

Steiner O, Coisne C, Engelhardt B, Lyck R. Comparison of immortalized bEnd5 and primary mouse brain microvascular endothelial cells as *in vitro* blood-brain barrier models for the study of T cell extravasation. J Cereb Blood Flow Metab 2011; 31: 315–27.

Ubogu EE, Cossoy MB, Ransohoff RM. The expression and function of chemokines involved in CNS inflammation. Trends Pharmacol Sci 2006; 27: 48–55.

Vajkoczy P, Laschinger M, Engelhardt B. Alpha4-integrin-VCAM-1 binding mediates G protein-independent capture of encephalitogenic T cell blasts to CNS white matter microvessels. J Clin Invest 2001; 108: 557–65.

Whitney LW, Becker KG, Tresser NJ, Caballero-Ramos CI, Munson PJ, Prabhu VV, et al. Analysis of gene expression in mutiple sclerosis lesions using cDNA microarrays. Ann Neurol 1999; 46: 425–8.

Zhao Y, Mangalmurti NS, Xiong Z, Prakash B, Guo F, Stolz DB, et al. Duffy antigen receptor for chemokines mediates chemokine endocytosis through a macropinocytosis-like process in endothelial cells. PLoS One 2011; 6: e29624.